Hindawi Publishing Corporation
Journal of Chemistry
Volume 2014, Article ID 245918, 6 pages
http://dx.doi.org/10.1155/2014/245918

Research Article

Preparation and Crystal Structures of Some $A^{IV}B_2{}^{II}O_4$ Compounds: Powder X-Ray Diffraction and Rietveld Analysis

K. Jeyadheepan[1,2] and C. Sanjeeviraja[1]

[1] *Department of Physics, Alagappa Chettiar College of Engineering and Technology, Karaikudi, Tamilnadu 630 004, India*
[2] *School of Electrical and Electronics Engineering, SASTRA University, Tirumalaisamudram, Thanjavur 613401, India*

Correspondence should be addressed to C. Sanjeeviraja; sanjeeviraja@rediffmail.com

Received 10 May 2013; Revised 13 December 2013; Accepted 16 December 2013; Published 2 February 2014

Academic Editor: Ali Nokhodchi

The $A^{IV}B_2{}^{II}O_4$ compounds such as cadmium tin oxide (Cd_2SnO_4 or CTO) and zinc tin oxide (Zn_2SnO_4 or ZTO) are synthesized by solid state reaction of the subsequent binary oxides. The synthesized powders were analyzed through the powder X-ray diffraction (PXRD). Cell search done on the PXRD patterns shows that the Cd_2SnO_4 crystallizes in orthorhombic structure with space group *Pbam* and the cell parameters as $a = 5.568(2)$ Å, $b = 9.894(3)$ Å, and $c = 3.193(1)$ Å and the Zn_2SnO_4 crystallizes as cubic with the space group $Fd\bar{3}m$ and with the cell parameter $a = 8.660(2)$ Å. Rietveld refinement was done on the PXRD patterns to get the crystal structure of the Cd_2SnO_4 and Zn_2SnO_4 and to define the site deficiency of atoms which causes the electrical properties of the materials.

1. Introduction

Conducting oxide materials are interested for several energy conversion applications, including solid state electrolytes for new types of storage and fuel cells, transparent electrode materials for some types of solar cells, and photo-electrolysis electrodes for the direct conversion of solar energy to hydrogen [1]. The $A^{IV}B_2{}^{II}O_4$ compounds such as Cd_2SnO_4 and Zn_2SnO_4 are important prototypes for modern high efficient transparent conducting oxides. The structure solution from powder X-ray diffraction and Rietveld refinement of some $A^{IV}B_2{}^{II}O_4$ compounds are reported where the group-II atoms are Mg, Zn, and Cd and group-IV atoms are Si, Ge, and Sn. But the structural studies of cadmium tin oxide (Cd_2SnO_4 or CTO) and zinc tin oxide (Zn_2SnO_4 or ZTO) lack a step in the literature.

Cadmium tin oxide was first synthesized by Smith [2] in 1960. Later, Nozik [3] studied its semiconducting properties and suggested it as a promising material for transparent electrodes. It has been reported that the oxygen vacancies in Cd_2SnO_4 provided the donor state for the conduction. Few coworkers [4, 5] suggested that the cadmium interstitials may also contribute to the conductivity. Zn_2SnO_4 was first prepared by Coffeen [6] through the wet chemical method, from its chemical precursors to precipitate the hydrated zinc stannates and followed by a sintering process at elevated temperatures, found to be an oxide semiconductor, and its crystal structure was determined to be cubic with inverse spinel ($MgAl_2O_4$) structure with the space group $Fd\bar{3}m$. Chang and Kaldon [7] have studied the solid state reaction of SnO_2-ZnO and observed that the solid state reaction between SnO_2 and ZnO is starting at above 1100°C, and Zn_2SnO_4 is the only resultant. Cun et al. [8] have studied the defect structure of Zn_2SnO_4 and suggested that the defect structure of Zn_2SnO_4 is mainly due to the oxygen deficiency with n-type conductivity.

Over the past decade, structure determination from powder diffraction (SDPD) has matured into a technique that is widely and successfully used in the context of organic, inorganic, and organometallic compounds [9]. By definition, the crystal belonging to the same structure type with same space group should have the similar cell parameters

and similar representative atom coordinates. But in the case of deficit materials like ternary compounds ($A^{IV}B_2{}^{II}O_4$ compounds) which have different atomic defects, have some major variations in the crystallographic parameters. Hence, the study of crystal structure of these compounds is necessary to understand its physical properties, especially the electronic properties. Hence, the present study aims at the preparation of Cd_2SnO_4 and Zn_2SnO_4 through the solid state reaction method and the determination of the structure of Cd_2SnO_4 and Zn_2SnO_4 powders through powder X-ray diffraction technique.

2. Experimental Details

The Cd_2SnO_4 powder was prepared from the solid state reaction of the well-blended mixture of required quantities of CdO (99.99% pure-Merck) and SnO_2 (99.99% pure-Merck) in the atomic weight ratio of 2 : 1. The mixed binary oxides, after making them as a 5 mm thick 50 mm diameter pellet, were kept at 1050°C for 6 hours in an autotuned, PID controlled SiC furnace at air atmosphere. The optimized time duration was selected based on the monophase compound formation which was confirmed through XRD results. The Zn_2SnO_4 powder was also prepared as mentioned above, from the well-blended mixture of the ZnO (99.99% pure-Merck chemicals) and SnO_2 (99.99% pure-Merck chemicals) in the atomic weight ratio of 2 : 1. The pellet was kept at 900°C in air for 4 hours. The temperature conditions were selected on the basis of thermal analysis results in both cases.

The TG/DTA analysis of the CdO-SnO_2 and the ZnO-SnO_2 mixed powders was made using TG/DTA analyzer (Perkin Elmer Diamond TGA/DTA). The instrument was calibrated using aluminum reference material which is having the transition point at 660.10°C. TG/DTA curves were measured in the constant flow of air at the rate of 10°C/min. X-ray diffraction analysis was made on the samples at room temperature using the PANalytical X'Pert PRO MPD diffractometer of the new generation equipped with two-dimensional solid state X'celerator detector. The data collection was done with 2θ ranging from 10 to 140° and the step width of 0.02° with 212 seconds per step counting time. Powder pattern indexing and the manual space group test were done in the software CMPR [10]; cell searching was done using TREOR 90 [11] algorithm. The Rietveld refinement was done using the GSAS [12] with EXPGUI [13] interface. Structural illustrations were obtained from DIAMOND [14] using the crystallographic information file (cif file). The materials for the publication were done in the EXPGUI itself. Raman spectrum of the Cd_2SnO_4 and Zn_2SnO_4 powders was recorded with the exciting laser wavelength of 480 nm.

The electrical conductivity, bulk carrier concentration, and the mobility of the samples were measured using the Ecopia Hall effect system model number HMS-3000 by making the powder as the hot pressed pellets.

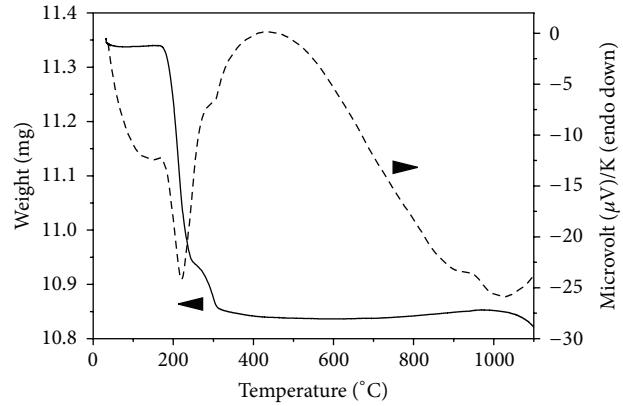

Figure 1: TG/TDA analysis of mixed precursor for Cd_2SnO_4.

3. Results

TG/DTA studies were made to study the temperature effect on the mixed sample of CdO and SnO_2 (sample 1) and also on the mixed sample of ZnO and SnO_2 (sample 2). The TG/DTA curves for the sample 1 are shown in Figure 1. In the TG curve, the multistage decomposition is observed at 210°C and 300°C. After the decomposition, a stable intermediate stage has been observed up to 900°C above which a slight increase in weight is observed up to 1050°C. Then, above 1050°C, another weight loss is observed. Figure 2 shows the TG/DTA analysis curve of the mixed sample of ZnO and SnO_2 (sample 2). In the TG curve of sample 2, rapid decomposition is observed sharply at 210°C. After the decomposition, a stable stage is observed approximately up to 725°C. After 725°C, a gradual increase in weight is observed up to 1000°C.

The prepared samples of Cd_2SnO_4 and Zn_2SnO_4 were subjected to the X-ray powder diffraction analysis with the step value of 0.02° to avoid the crystallographic analysis errors. Manual cell search done on the Cd_2SnO_4 sample in CMPR using the TREOR90 algorithm revealed that the Cd_2SnO_4 powder crystallized in orthorhombic structure with cell parameters $a = 5.568$ Å, $b = 9.894$ Å, and $c = 3.193$ Å and cell volume as 175.94 Å^3 with the figure of merit (FOM) of 62.0. Space group test, done with the peak positions, reveals that the space group is *Pbam* (55). Cell search done on the Zn_2SnO_4 sample deduced that the Zn_2SnO_4 powder crystallized in cubic structure with cell parameter $a = 8.660$ Å and the cell volume as 649.27 Å^3 with the FOM of 61. Space group test done, with the peak positions only, reveals that the space group is $Fd\bar{3}m$ (227).

Figure 3 shows the Rietveld refinement plot of Cd_2SnO_4 powder diffraction data. The difference plot and the plot of cumulative χ^2 value show the convergence of the Rietveld refinement. The crystal and experimental data of the Rietveld refinement is given in Table 1. Figure 4 shows the Rietveld refinement plot of Zn_2SnO_4 powder diffraction data. The crystal and the Rietveld refinement data of Zn_2SnO_4 is given in Table 2.

Figures 5 and 6(a) show the schematic representations of the crystal structures of the orthorhombic Cd_2SnO_4 and

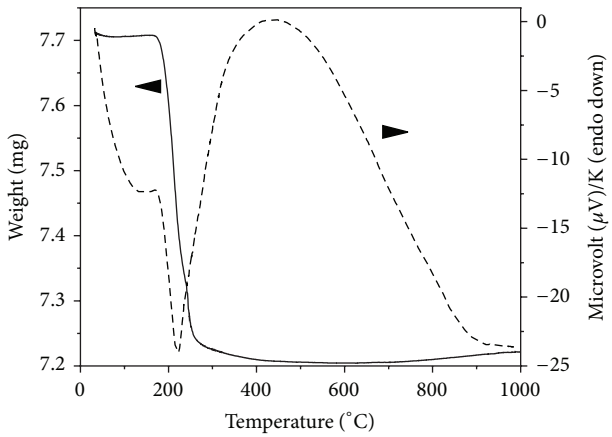

Figure 2: TG/DTA analysis curve of mixed precursors for Zn_2SnO_4.

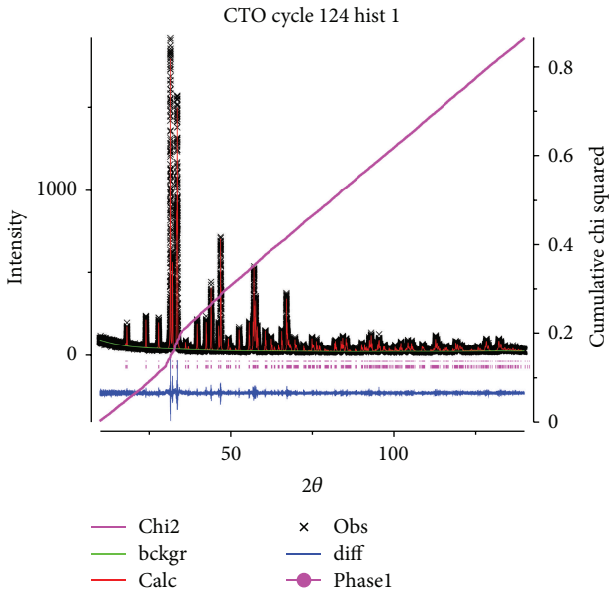

Figure 3: Rietveld refinement plot of Cd_2SnO_4.

Table 1: Crystal and refinement data of Cd_2SnO_4.

Empirical formula: Cd_2SnO_4	
Chemical formula: $Cd_{3.58}Sn_{1.78}O_{8.05}$	
Formula weight: 741.99	
Wavelength: $K_{\alpha1}$ = 1.54060 Å; $K_{\alpha2}$ = 1.5444 Å	
Temperature: 300 K	
Crystal system: orthorhombic	
Space group: *Pbam* (55)	$Z = 1$
a = 5.568(2) Å	$\alpha = \beta = \gamma = 90^\circ$
b = 9.894(4) Å	
c = 3.193(12) Å	
V = 175.96(10) Å^3	
D_x = 7.002 g/cm^3	
No. of reflections used = 394	
$2\theta_{min} = 10.00^\circ$, $2\theta_{max} = 140.00^\circ$	
R_p = 0.105	
R_{wp} = 0.145	
R_{exp} = 0.155	
R = 0.0407	
Reduced χ^2 = 0.867	
S = 0.93	
$(\Delta/\sigma)_{max}$ = 0.02	
No. of parameters = 82	
Least squares matrix: full	
No. of cycles = 124	
Crystallite size = 156.73 nm	
Strain = 0.094 × 10^{-3}	

Table 2: Fractional atomic coordinates and isotropic displacement parameters of Cd_2SnO_4 (in Å).

Atom	Site	X	y	z	Uiso*/Ueq	Occ. (<1)
Sn1	*2a*	0	0	0	0.0032(27)	0.890(4)
Cd2	*4h*	0.0585(10)	0.3224(7)	0.5	0.0057(22)	0.893(33)
O3	*4h*	0.2369(9)	0.0418(5)	0.5	0.0100(21)	0.994(20)
O4	*4g*	0.3620(10)	0.3052(6)	0	0.0230(25)	1.019(18)

cubic spinel Zn_2SnO_4, respectively. Figures 6(b) and 6(c) show the octahedrally and tetrahedrally coordinated cations, respectively.

Raman spectrum of the Cd_2SnO_4 and Zn_2SnO_4 powders is shown in Figures 7 and 8, respectively. In Figure 7, the strong Raman shift peaks at 605.9 cm^{-1}, 548 cm^{-1}, and 474.6 cm^{-1} correspond to the Cd_2SnO_4 peaks [14]. In Figure 8, strong Raman shift peaks at 670.3 cm^{-1} and 527.8 cm^{-1} correspond to the well-known ZTO peaks [15].

The conductivity of the prepared Cd_2SnO_4 is 2.095 × 10^3 S/cm with the bulk concentration 4.439 × 10^{20} cm^{-3} and the mobility 29.46 cm^2/Vs and the conductivity of the Zn_2SnO_4 is 65.38 S/cm with bulk concentration 5.375 × 10^{18} cm^3 and the mobility 7.592 cm^2/Vs.

4. Discussion

In the TG curve of Figure 1, the initial mass loss observed up to 100°C is characteristics of desorption or drying of the mixed CdO and SnO_2 powders. The multistage decomposition at 207°C and 300°C may be attributed to the ionization of excess of Cd and Sn present in the CdO and SnO_2, respectively. After the decomposition, a stable intermediate stage has been observed up to 900°C above which a slight increase in weight indicates the oxidation of the sample at higher temperature [16]. At about 1050°C, the observed weight indicates an oxidative decomposition reaction again at higher temperature. The sharp peaks observed in DTA curve at 210°C and 300°C reveal the purity of the precursors taken. From TG/DTA analysis, it is clear that, above 1000°C, the oxidation takes place. So the mixed sample, after making it

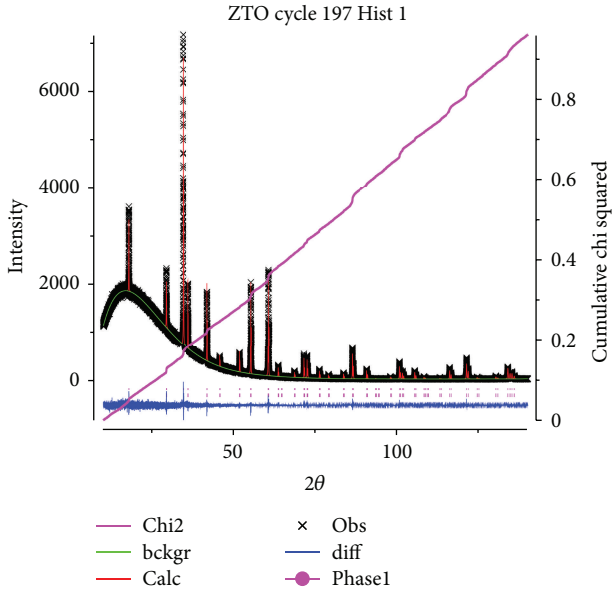

Figure 4: Rietveld refinement plot of Zn_2SnO_4.

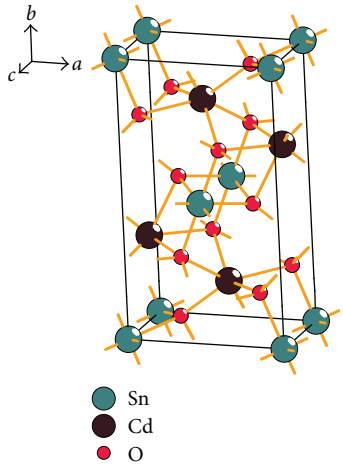

Figure 5: Schematic representation of the crystal structure of orthorhombic Cd_2SnO_4.

as a 5 mm thick 50 mm diameter target, was kept at 1050°C for 6 hours in air.

In the TG/DTA curve of Zn_2SnO_4 precursor, there are only two weight loses present in the TG curve. According to Cun et al. [17], a weight loss observed at about 120°C may be attributed to the liberation of the surface-adsorbed water and another weight loss at about 210°C might be attributed to the liberation of the crystal water. There is no any recrystallization taking place at about 724°C. Only a constant intermediate phase is observed. The gradual increase in weight observed above the 725°C may be attributed to the oxidation of the Zn_2SnO_4 precursor. This oxidation is observed up to 1000°C also. So the precursor, after making it as a 5 mm thick 50 mm diameter target, was kept at 950°C for 6 hours in air atmosphere.

Table 3: Crystal and refinement data of Zn_2SnO_4.

Empirical formula: Zn_2SnO_4	
Chemical formula: $Zn_{60.53}Sn_{36.12}O_{138.74}$	
Formula weight: 10463.77	
Wavelength: $K_{\alpha1}$ = 1.54060 Å; $K_{\alpha2}$ = 1.5444 Å	
Temperature: 300 K	
Crystal system: cubic	
Space group: $Fd\,\bar{3}\,m$ (227)	$Z = 1$
a = 8.6604(2) Å	$\alpha = \beta = \gamma = 90^\circ$
V = 649.56(5) Å^3	
D_x = 26.75 g/cm^3	
No. of reflections used = 90	
$2\theta_{min} = 10.00^\circ$, $2\theta_{max} = 140.00^\circ$	
R_p = 0.03	
R_{wp} = 0.051	
R_{exp} = 0.052	
R = 0.034	
Reduced χ^2 = 0.959	
S = 0.98	
$(\Delta/\sigma)_{max}$ = 0.01	
No. of parameters = 21	
Least squares matrix: full	
No. of cycles = 197	
Crystallite size = 253.39 nm	
Strain = 0.626 × 10^{-3}	

The cadmium stannate may be crystallized as monocadmium stannate ($CdSnO_3$) or dicadmium stannate which are of the same orthorhombic structure. To avoid the wrong indexing problem due to the same crystal structure, high quality powder diffraction data is needed. Hence, the powder X-ray diffraction analysis was done on the samples with the 2θ step value of 0.02°. Since the powder diffraction data is of high quality, the highest FOM values of 62 for Cd_2SnO_4 and 61 for Zn_2SnO_4 were achieved.

In the crystallographic analysis, the possibility of the monocadmium stannate ($CdSnO_3$) was also checked and the results showed that the space group *pnma,* which is for $CdSnO_3$, has the figure of merit of 5.6637 with 10 unexplained lines. Hence, it is confirmed that the orthorhombic Cd_2SnO_4 is the only product in the solid state reaction of CdO, and SnO_2 in the ratio of 2 : 1 at the temperature of 1050°C, as the orthorhombic structure is mostly favored for bulk Cd_2SnO_4 [18]. There are no any secondary phases like $CdSnO_3$, CdO or SnO_2. Characteristic peaks obtained in the Raman spectrum also confirm the Cd_2SnO_4 formation. The broadening and asymmetry of the peaks indicate the typical features of the nanoscale materials which supports the crystallite size results of XRD.

The result of the Rietveld refinement of Cd_2SnO_4 is given in Table 1. Fractional atomic coordinates and isotropic displacement parameters of Cd_2SnO_4 are given in Table 2. The Rietveld refinement was done with manual background fitting and with the pseudo-Voigt profile function. The least square refinement was converged with the R value of 0.0407

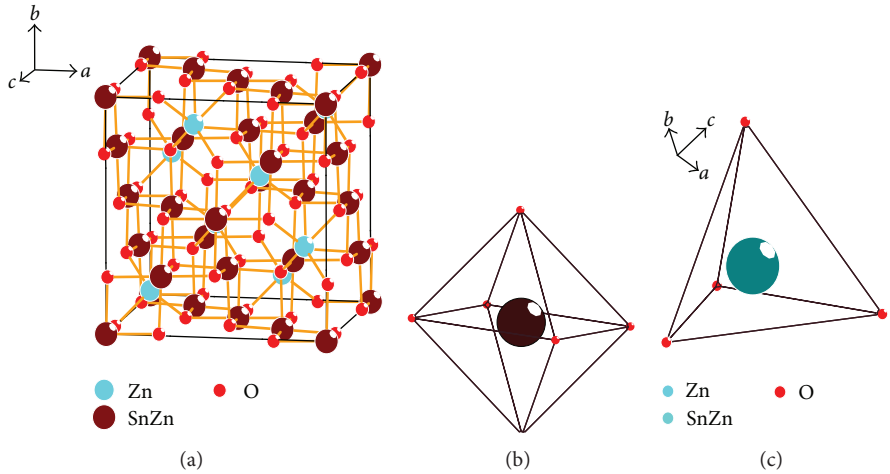

FIGURE 6: (a): Schematic representation of the crystal structure of "inverse spinel" Zn_2SnO_4. (b) Octahedrally coordinated "SnZn" cation. (c) Tetrahedrally coordinated Zn atom.

TABLE 4: Fractional atomic coordinates and isotropic displacement parameters of Zn_2SnO_4 (in Å).

Atom	Site	X	y	z	Uiso*/Ueq	Occ. (<1)
Zn1	*16c*	0.0	0.0	0.0	0.0151*	1.714 (21)
Zn2	*8b*	0.375	0.375	0.375	0.0085*	4.138 (20)
Sn3	*16c*	0.0	0.0	0.0	0.0246*	2.26
O4	*32e*	0.2416 (13)	0.2416 (13)	0.2416 (13)	0.0130*	4.336 (26)

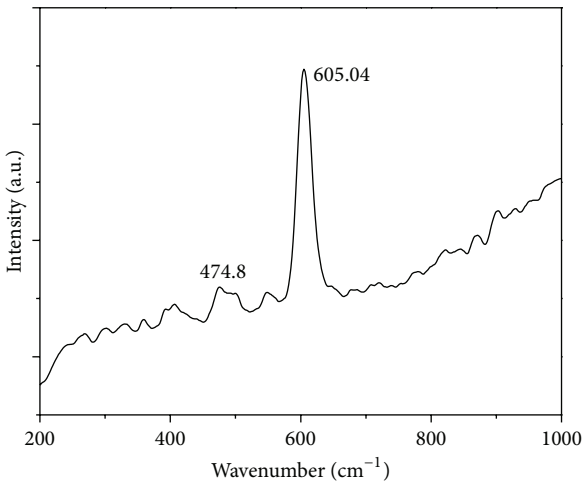

FIGURE 7: Raman spectrum of Cd_2SnO_4 powder.

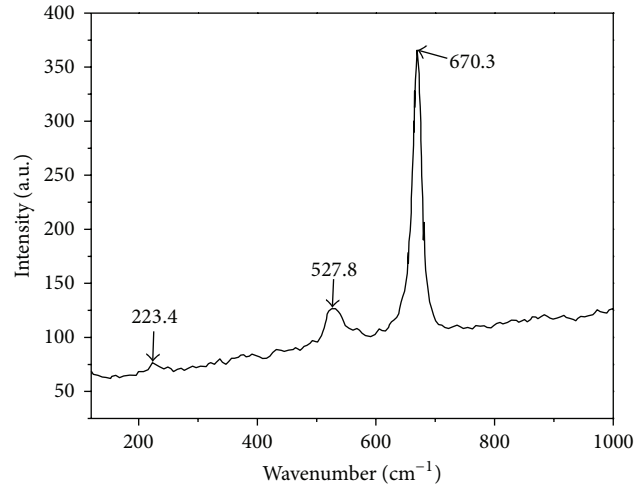

FIGURE 8: Raman spectrum of Zn_2SnO_4 powder.

with R_p value of 0.105, χ^2 of 0.8675, and the goodness of fit (GOF) of 0.93. The values of χ^2 and GOF confirm the best fit of the calculated profile function to the observed diffraction data. The weight ratio of Cd, Sn, and O (given in Table 1) reveals that there is no any oxygen vacancy in the compound to contribute to the conductivity. The excess proportion of Cd atom shows that the Cd interstitials only contribute to the high conductivity which pronounced the high conductivity value of 2.095×10^3 S/cm. Since there is no any disorder in the site of cations (Cd and Sn), the mobility will be increased to the value of 29.46 cm^2/Vs, even though there is the high bulk carrier concentration of 4.439×10^{20} cm^{-3}. It makes the normal orthorhombic Cd_2SnO_4 more conductive in nature than the cubic spinel structure.

Approximate fractional atomic coordinates found from the structure refinement show that the tetrahedral voids (*8b*) are occupied by Zn atoms and the octahedral voids (*16c*) are occupied randomly by an equal number of Zn and Sn atoms [19] which confirms the inverse spinel structure of the Zn_2SnO_4 in which the Zn_2SnO_4 is more stable [18]. The

Rietveld refinement was converged with the R value of 0.034, R_p value of 0.030, R_{wp} of 0.051, and reduced χ^2 value of 0.959. The crystallographic and refinement data of Zn_2SnO_4 were given in Table 3. The atomic coordinates and the isothermal displacement parameters were given in Table 4. The weight ratio of the Zn_2SnO_4 given in Table 3 reveals that the oxygen vacancy (V_o) is the main reason for the conductivity of Zn_2SnO_4 to the value of 65.38 S/cm. Normally, Zn_2SnO_4 is composed of closely packed oxygen ions and rutile chains which are connected by cations in the tetrahedral sites and which run through the lattice. The rutile chains are considered as conduction paths for electrons as unoccupied orbital of cations which significantly overlap in the chains because of short cation-cation separation distances due to the edge sharing of cation octahedra. But the spinel lattice of Zn_2SnO_4 is locally distorted enough to form two distinct octahedrally coordinated Sn and Zn sites. The disorder in the Sn and Zn sites in the lattice significantly limits the mobility of the carriers (7.592 cm^2/Vs), possibly by disrupting the edge-sharing nature of the octahedrally coordinated cations [20]. The characteristic Raman peaks confirm the Zn_2SnO_4 formation.

5. Conclusion

The accurate X-ray structural investigations of orthorhombic Cd_2SnO_4 and cubic inverse spinel Zn_2SnO_4 and the use of the experimental data with high resolution of $\Delta 2\theta = 0.02^\circ$ allowed us to obtain the results with high relative precision (reduced $\chi^2 \sim 1$). As the inclusion of a large number of high angle weak reflections in the analysis leads to a decrease in accuracy of the results of the refinement, the design and the performance of the experiment and the methods used to process the experimental data made it possible to overcome the influence of this factor. The electrical conductivity and the mobility values were correlated with the site occupancy, atomic site defects, and also the weight percentage of the element present in the compounds.

Conflict of Interests

The author(s) declare(s) that there is no conflict of interests regarding the publication of this paper.

References

[1] K. J. D. Mackenzie, W. A. Gerrard, and F. Golestani-Fard, "The electrical properties of monocadmium and dicadmium stannates," *Journal of Materials Science*, vol. 14, no. 10, pp. 2509–2512, 1979.

[2] A. J. Smith, "The system cadmium oxide-stannic oxide," *Acta Crystallographica*, vol. 13, pp. 749–752, 1960.

[3] A. J. Nozik, "Optical and electrical properties of Cd_2SnO_4: a defect semiconductor," *Physical Review B*, vol. 6, no. 2, pp. 453–459, 1972.

[4] B. Li, L. Zeng, and F. Zhang, "Structure and electrical properties of $CdIn_2O_4$ thin films sputtered at elevated substrate temperatures," *Physica Status Solidi (A)*, vol. 201, no. 5, pp. 960–966, 2004.

[5] T. J. Coutts, D. L. Young, X. Li, W. P. Mulligan, and X. Wu, "Search for improved transparent conducting oxides: a fundamental investigation of CdO, Cd_2SnO_4, and Zn_2SnO_4," *Journal of Vacuum Science and Technology A*, vol. 18, no. 6, pp. 2646–2660, 2000.

[6] W. W. Coffeen, "Ceramic and dielectric properties of the stannates," *Journal of the American Ceramic Society*, vol. 36, pp. 207–214, 1953.

[7] L. L. Y. Chang and R. C. Kaldon, "Phase relations in the systems MgO-ZnO-SnO_2, NiO-ZnO-SnO_2, and MgO-NiO-SnO_2," *Journal of the American Ceramic Society*, vol. 59, pp. 275–277, 1976.

[8] W. Cun, W. Xinming, Z. Jincai et al., "Synthesis, characterization and photocatalytic property of nano-sized Zn_2SnO_4," *Journal of Materials Science*, vol. 37, pp. 2989–2996, 2002.

[9] W. I. F. David, K. Shankland, L. B. McCusker, and Ch. Baerlocher, "Introduction," in *Structure Determination from Powder Diffraction Data*, W. I. F. David, K. Shankland, L. B. McCusker, and Ch. Baerlocher, Eds., pp. 1–11, Oxford University Press, New York, NY, USA, 2002.

[10] B. H. Toby, "*CMPR*—a powder diffraction toolkit," *Journal of Applied Crystallography*, vol. 38, pp. 1040–1041, 2005.

[11] P. E. Werner, L. Erikson, and M. Westdahl, "*TREOR*, a semi-exhaustive trial-and-error powder indexing program for all symmetries," *Journal of Applied Crystallography*, vol. 18, pp. 367–370, 1985.

[12] A. C. Larson and R. B. von Dreele, "General structure analysis system (GSAS)," Los Alamos National Laboratory Report LAUR 86-748, 2004.

[13] B. H. Toby, "EXPGUI, a graphical user interface for GSAS," *Journal of Applied Crystallography*, vol. 34, no. 2, pp. 210–213, 2001.

[14] *Diamond—Crystal and Molecular Structure Visualization*, Crystal Impact—K. Brandenburg & H. Putz GbR, Bonn, Germany.

[15] C. Ronconi and O. L. Alves, "A Study on the formation of a porous morphology in Cd_2SnO_4 thin films prepared by mod process," *Molecular Crystals and Liquid Crystals*, vol. 374, no. 1, pp. 275–280, 2002.

[16] M. E. Brown, *Introduction to Thermal Analysis: Techniques and Applications*, Kluwer Academic, Amsterdam, The Netherlands, 2nd edition, 2001.

[17] W. Cun, W. Xinming, Z. Jincai et al., "Synthesis, characterization and photocatalytic property of nano-sized Zn_2SnO_4," *Journal of Materials Science*, vol. 37, no. 14, pp. 2989–2996, 2002.

[18] D. Segev and S.-H. Wei, "Structure-derived electronic and optical properties of transparent conducting oxides," *Physical Review B*, vol. 71, no. 12, Article ID 125129, 11 pages, 2005.

[19] S.-H. Wei and S. B. Zhang, "First-principles study of cation distribution in eighteen closed-shell $A^{II}B_2^{III}O_4$ and $A^{IV}B_2^{II}O_4$ spinel oxides," *Physical Review B*, vol. 63, no. 4, Article ID 045112, 8 pages, 2001.

[20] D. L. Young, D. L. Williamson, and T. J. Coutts, "Structural characterization of zinc stannate thin films," *Journal of Applied Physics*, vol. 91, no. 3, pp. 1464–1471, 2002.